Received August 8, 2017, accepted September 7, 2017, date of publication September 13, 2017, date of current version April 23, 2018.

Digital Object Identifier 10.1109/ACCESS.2017.2751620

A New Approach to Iterative Clipping and Filtering PAPR Reduction Scheme for OFDM Systems

KELVIN ANOH[1], (Member, IEEE), CAGRI TANRIOVER[2], BAMIDELE ADEBISI[1], (Senior Member, IEEE), AND MOHAMMAD HAMMOUDEH[1]

[1]School of Engineering, Manchester Metropolitan University, Manchester, M1 5GD, U.K.
[2]Intel Labs, OR 97124, USA

Corresponding author: Kelvin Anoh (k.anoh@mmu.ac.uk)

This work was supported by EPSRC through the Peer-to-Peer Energy Trading and Sharing–3M (Multi-times, Multi-scales, Multi-qualities) Project under Grant EP/N03466X/1.

ABSTRACT While achieving reduced/good peak-to-average power (PAPR) in orthogonal frequency division multiplexing (OFDM) systems is attractive, this must not be performed at the expense of the transmitted signal with over-reduced signal power, as it leads to degraded bit error ratio (BER). We introduce a uniform distribution approach to solving the PAPR reduction problem of OFDM signals and then use Lagrange multiplier (LM) optimization to minimize the number of iterations involved in an adaptive fashion. Due to the nonlinear attenuation of the PAPR reduction scheme, we compensate the output signal using a correlation factor that minimizes the error floor in the in-band distortion of the clipped signal using the minimum mean square error method so as to improve the BER performance. Three different methods are introduced each enabling PAPR reduction by clipping followed by filtering with no direct dependence on a clipping ratio parameter. We find that our approach significantly reduces the PAPR of the OFDM signals (especially with LM optimization) better than the conventional adaptive iterative clipping and filtering operating without LM optimization. Based on our proposed methods, we additionally outline two simple steps for achieving perfect PAPR reduction (i.e., 0 dB). We also evaluate the performance of the three new models over high power amplifier (HPA) for completeness; the HPA is found to induce negligible BER degradation effects on the processed signal compared with the unprocessed signal.

INDEX TERMS OFDM, iterative clipping and filtering (ICF), adaptive ICF, PAPR, optimization, Lagrange multiplier, uniform distribution, high power amplifier (HPA).

I. INTRODUCTION

Orthogonal frequency division multiplexing (OFDM) is an efficient multicarrier communication style over fading channels since the narrow-bandwidths subtended in the frequency domain allow long symbol period. This property provides protection against channel impulse response effects and makes OFDM attractive in the design of modern communication systems for efficient management of scarce radio frequency bandwidths. Further spectral efficiency can be achieved by using wavelets which can operate OFDM without cyclic prefix [1], [2]. Unfortunately, high peak-to-average power ratio (PAPR) problem limits its wide adoption in some communication devices. For example, while OFDM is applied in downlink transmissions of mobile communication standards, it is not preferred in uplink transmissions due to PAPR limitation [3]. High PAPR leads power amplifiers to operate in the saturation region expending large system power and induces bit error ratio (BER) degradation due to smearing of signals.

In the literature, different PAPR reduction techniques exist and may be applied before or after OFDM modulation [4]. Two families of post-modulation PAPR reduction schemes include companding and clipping [4]–[7]. Companding destroys the orthogonality of OFDM subcarriers and may cause the signals to be unrecoverable at the receiver. Clipping does not require receiver-side processing, thus reduces the receiver-side complexity unlike companding. In this study, we focus on iterative clipping and filtering (ICF) technique although the conventional ICF PAPR reduction technique has been around for some time [6].

ICF is attractive because it is simple to implement, achieves better power amplifier efficiency at the cost of increasing in-band distortion while restricting out-of-band power radiation due to power amplification [8] and can be designed to achieve good BER performances [9]–[11]. After the introduction of clipping and filtering by [6], many studies [3], [4], [8]–[10], [12], [13] have been done to perfect the technique as an ideal post-multicarrier modulation PAPR reduction method for OFDM systems. However, all these schemes are based on specifying a clipping ratio.

In this study, a different approach that does not require a predefined clipping ratio is taken. This approach is based on the fact that transforming the amplitude distribution to a uniform distribution can lead to perfect PAPR reduction; thus we establish the steps for achieving such distribution through clipping. At this stage, let us first recapitulate that conventional OFDM signal has characteristic amplitude distribution that follows Rayleigh distribution. The amplitudes distributed above the mean are fundamentally responsible for high PAPR problem and drive the high power amplifier (HPA) towards saturation region where it consumes large amount of power and smears the signals thereby degrading the BER. Due to the dynamic and unique nature of each OFDM symbol and the amplitudes, we explore the realization of a uniform distribution by ICF without using the conventional predetermined clipping ratio.

Companding is the foremost PAPR reduction scheme that explicitly imposes uniform distribution probability density function (PDF) constraint unto the Rayleigh PDF of the conventional OFDM signal amplitudes (e.g. [7], [14], [15]). However, companding destroys the orthogonality of the subcarriers, unfairly expands the low amplitude signals or compresses the larger amplitude signals - due to amplitude distortion, these increase noise overhead and lead to poor BER performance.

We propose the possibility of addressing PAPR problem by clipping without setting thresholds. For example, if the signal amplitude peaks can be made to approach a uniform distribution, then the PAPR problem can also be eliminated. Unlike converting the PDFs by using different companding transforms, we restrict our design to the mean amplitude distribution. For example, we estimate the mean amplitude of OFDM signals, then clip all other amplitudes higher than the mean amplitude; this we called Method 1. We found that this greatly reduced the PAPR of the system by 10dB and 11dB in 1 and 3 iterations, respectively. As there are many subcarriers exhibiting the characteristic amplitudes higher than the mean amplitude, this led to high in-band distortion which adversely impacted the BER performance.

Since the BER is greatly degraded, we further introduced another method that can improve the BER at the expense of the PAPR. This was achieved by scaling up the mean amplitude so that the number of clipped signals is reduced thus reducing the in-band distortion; this we called Method 2. We compared both the PAPR performances of Method 2 with the original signal and observed that Method 2 reduced the PAPR of unclipped OFDM signal by 9.5dB. In terms of the BER, Method 2 achieved 3.4dB gain over Method 1. Method 2 is attractive since convergence after 1 iteration achieves good (PAPR and BER) level, which offers a good trade-off in terms of processing time and power consumption required for running $2M+1$ IFFT/FFT operations (where 'M' is the number of iterations).

We emphasize that the two approaches do not require any predetermination of clipping ratio as it is the custom of the conventional ICF. Based on these two methods, it follows that the PAPR problem can be completely eliminated by two simple steps, which leads us to a third method, namely Method 3; 1) determine the signal amplitudes below the mean and scale them up using the approach in Method 2, to transform these lower energy signals to equal or higher amplitudes as the mean signals; 2) determine the amplitudes distributed above the mean, then clip the excess - this achieves the complete PAPR reduction to 0dB.

However, to reduce the number of iterations involved, we apply the Lagrange multiplier (LM) optimization technique to reduce the distortion noise which further reduced the PAPR by another 3.5dB so that the unclipped OFDM signal PAPR is reduced by 11.5dB in 3 iterations only using Method 1 and to 0dB in Method 3. We also measured the amount of out of band emissions generated by our approach and realized 4.47dB, 1.68dB and 3.23dB gains for Methods 1, 2 and 3 respectively when compared with the results of unclipped signals.

II. PROPOSED ICF MODEL

At baseband, the discretely sampled OFDM symbols at the Nyquist rate do not exhibit equivalent PAPR as the continuous symbols, thus oversampling is usually required [5], [16]. Given an oversampled frequency domain OFDM signal,

$$X = \left[\underbrace{d_0, d_1, \cdots, d_{N-1}}_{\text{input data}}, \underbrace{0, 0, \cdots, 0_{N(\ell-1)}}_{\text{oversampling zeros}}\right],$$

as shown in Fig. 1, it can be converted to a time-domain after oversampling as follows

$$\boldsymbol{x}(n) = \frac{1}{\sqrt{\ell N}} \sum_{k=0}^{\ell N-1} X(k) e^{j2\pi \frac{kn}{\ell N}} \quad \forall n = 0, 1, \cdots, \ell N - 1 \tag{1}$$

where ℓ is an oversampling factor, usually $\ell \geq 4$, $j = \sqrt{-1}$ and N is the number of data symbols and ℓN is the number over-sized subcarriers after oversampling. Since the $x(n)$ is characteristically complex with real $\boldsymbol{x}_r(n)$ and imaginary $\boldsymbol{x}_i(n)$ components, the amplitude of the signal can be calculated as

$$|\boldsymbol{x}(n)| = \sqrt{\boldsymbol{x}_r(n)^2 + \boldsymbol{x}_i(n)^2} \tag{2}$$

From (2), it can be shown as illustrated in Fig. 2 that OFDM signal has amplitude distribution that follows Rayleigh distribution since $\boldsymbol{x}_r(n)$ and $\boldsymbol{x}_i(n)$ are independently and identically

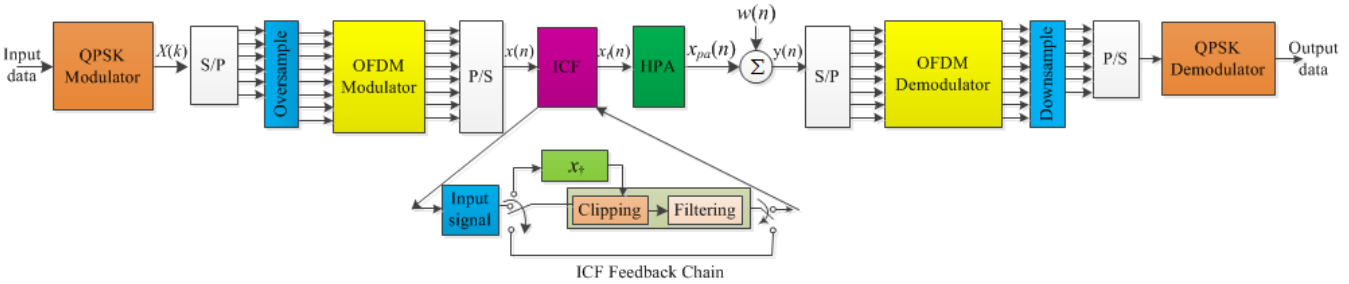

FIGURE 1. OFDM system model showing ICF technique for PAPR reduction; ICF block envelopes the adaptive ICF solution implemented with Lagrange multiplier optimization to reduce clipping and filtering iterations.

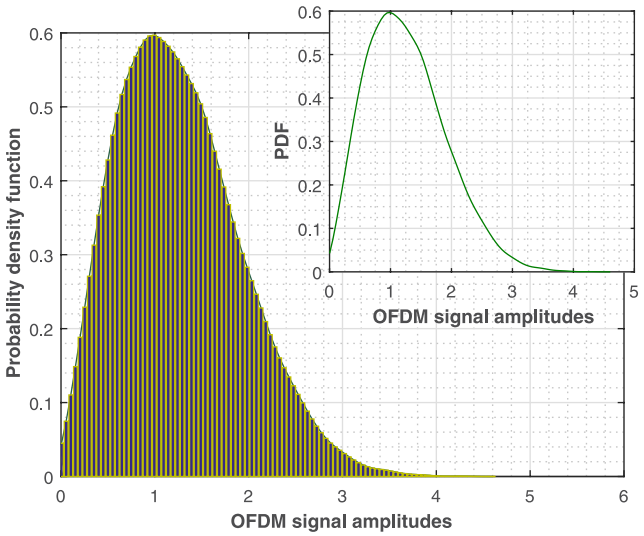

FIGURE 2. PDF distribution of OFDM signal demonstrating the amplitude distribution which influences the PAPR behaviour of the system.

distributed Gaussian random variables according to central limit theorem. Being Rayleigh distributed as in Fig. 2 suggests that the small fraction of amplitudes distributed above the mean amplitude lead to high PAPR problem.

Our goal is to convert the amplitude distribution, by clipping, to achieve a uniform distribution. However, the conventional ICF scheme is usually limited to a preset clipping threshold and clipping ratio; this limits how much PAPR that be can reduced. It also requires many iterations [10], [17] which expends the system power and expands the processing time. A way of overcoming these limitations is by making the clipping threshold adaptive as described in [13] while another is by constructing a PAPR reduction vector [9]. Motivated by the fact that OFDM symbols are dynamic with varying amplitude distribution and the studies presented in [9] and [13], we propose a technique that does not require the clipping ratio and threshold limitations in this study. For example, recall the conventional ICF method, usually defined as [8]

$$\hat{\boldsymbol{x}}(n) = \begin{cases} T \times \exp\left(j \times \theta_n\right), & |\boldsymbol{x}(n)| > T \\ \boldsymbol{x}(n), & |\boldsymbol{x}(n)| \leq T \end{cases} \tag{3}$$

where T is the desired amplitude derived from $T = \gamma_o \sqrt{P_{av}}$, γ_o is the clipping ratio and $P_{av} = \frac{1}{\ell N} \sum_{n=0}^{\ell N-1} |x(n)|^2$, $\theta_n = \arg\{\boldsymbol{x}(n)\}$ is the phase of $\boldsymbol{x}(n)$ and $\hat{\boldsymbol{x}}(n)$ is the output clipped signal. From (3), we emphasize that clipping PAPR reduction technique is amplitude-based PAPR scheme and does not impact the phase of the signal. Besides, to remove the in-band distortion noise arising from excess clipped signals, a frequency domain filtering is applied. This leads to peak regrowth and increases the PAPR. To cushion this effect, the clipping is repeated a few times until the desired PAPR is achieved.

In the adaptive case [13], the authors argue that T must be recalculated based on the output amplitude of $\hat{\boldsymbol{x}}(n)$ instead of the hard-fixed threshold which improved the PAPR performance. However, an OFDM signal frame is characterized by three different amplitudes [18], namely

$$x_\dagger = \frac{1}{\ell N} \sum_{n=0}^{\ell N-1} |x(n)| \tag{4a}$$

$$x_{min} = \underset{x_{n=0,\cdots,\ell N-1}}{\arg} \min\{|x(n)|\} \tag{4b}$$

$$x_{max} = \underset{x_{n=0,\cdots,\ell N-1}}{\arg} \max\{|x(n)|\} \tag{4c}$$

In general, we can also summarize (4) into a vector of the form

$$|x(n)| = \left[|x(n)| < x_\dagger,\ x_\dagger,\ |x(n)| > x_\dagger\right], \quad \forall n = 0, 1, \cdots, \ell N - 1. \tag{5}$$

If (4a) is seen as the average power signals, then (4c) and (4b) are the high and low power signals, respectively. A sister approach to ICF, namely companding, expands the energy of the low amplitude signals [19] or simultaneously compresses and expands the amplitude of (4c) and (4b) to achieve PAPR reduction [7]. One of the notable companding examples [14], [20] can be said to have derived from (4), segmenting the characteristic amplitudes of (1) into (4a), (4b) and (4c) to construct an amplitude transforming PDF model that converts Rayleigh distribution into a near-uniform distribution. The trapezoidal distribution [14], [20] followed in that discussion leads to the unsolved PAPR problem as the realized distribution is non-uniform due to the central peak. These methods present some exploitative insights yet unexplored with the use of ICF PAPR reduction style.

Now, we summarize the PAPR problem in OFDM systems to avoid non-uniformly distribution of signal amplitudes. In order to make these peaks uniformly distributed, we clip the amplitudes $\left(|x(n)| > x_{\dagger}\right)$ within the upper bound of (5). Consequently, we restate the ICF solution in (3) as

$$\hat{\boldsymbol{x}}(n) = \begin{cases} x_{\dagger} \times \exp\left(j \times \theta_n\right), & |\boldsymbol{x}(n)| > x_{\dagger} \\ \boldsymbol{x}(n), & |\boldsymbol{x}(n)| \leq x_{\dagger} \end{cases} \tag{6}$$

Considering the other two characteristic amplitudes of an OFDM system in (4), choosing x_{min} in (4b) to determine the clipped signal will reduce the energy in the signals to mere noise and will be severely attenuated/convolved with the in-band distortion from the excess amplitudes to become irrecoverable at the receiver. On the other hand, choosing x_{max} in (4c) will be too large that nothing will be clipped and will also lead to smearing at HPA degrading BER and causing the HPA to expend more power. In Fig. 3, we exemplify the amplitude distribution of the clipped signal for large number of subcarrier $N = 1024$ with $\ell = 4$.

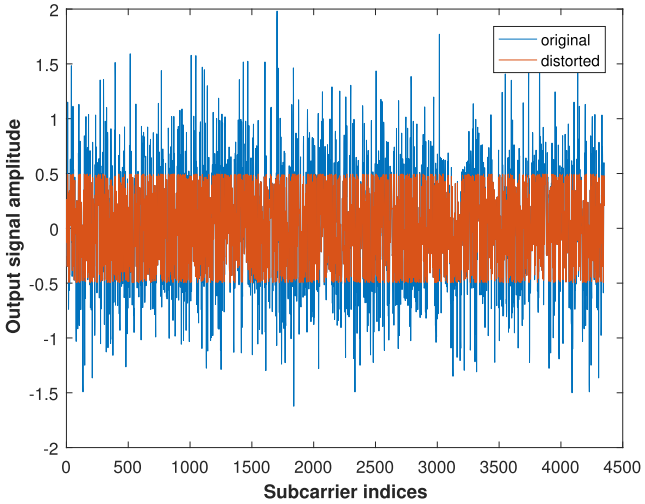

FIGURE 3. Amplitude distribution of conventional OFDM signals compared to the clipped signals using the proposed scheme.

From Fig. 3, the clipped signals are nicely uniformly distributed, $U\left(-x_{\dagger}, x_{\dagger}\right)$. This will significantly reduce the PAPR as it will be demonstrated shortly in Section IV. However, since large number of these signals are distorted the consequential effect is high in-band distortion leading to poor BER performance. Thus, filtering must be applied to restore the BER performance of the system by removing the in-band distorting components. The above ICF model is referred to as Method 1 in this work.

A. PROPOSED ICF MODEL (METHOD 2 - UP SCALING THE MEAN AMPLITUDE)

Recall the characteristic amplitudes of an OFDM signal described in (4), then, comparing (4c) and (4a) as

$$\Delta x = x_{max} - x_{\dagger} \tag{7}$$

depicted in Fig. 3, it can be observed that Δx is large. A way of reducing (7) is by scaling up (4a) with respect to the excess amplitude in Fig. 3 (i.e. Δx) as follows

$$x_{\dagger\ddagger} = \sqrt{\frac{\ell N}{P}} x_{\dagger} \tag{8}$$

where P is from

$$x(p) = |\boldsymbol{x}(n)| > x_{\dagger}, \quad \forall n = 1, \cdots, \ell N \; \forall p = 1, \cdots, P \tag{9}$$

In other words, P is the number of elements in $\boldsymbol{x}(0 \leq p \leq P-1)$. Now, by casting (8) unto (6) substituting for $x_{\dagger}$, we express the new clipping criteria as

$$\hat{\boldsymbol{x}}(n) = \begin{cases} x_{\dagger\ddagger} \times \exp\left(j \times \theta_n\right), & |\boldsymbol{x}(n)| > x_{\dagger\ddagger} \\ \boldsymbol{x}(n), & |\boldsymbol{x}(n)| \leq x_{\dagger\ddagger} \end{cases} \tag{10}$$

The ideal of the second approach is that although the amplitudes are selectively increased, however, these increases are not within the nonlinear region of the HPA and thus avoids nonlinear smearing (distortion) of the amplitudes of the input signals which would lead to good BER performance as it will be illustrated in Section IV-B.

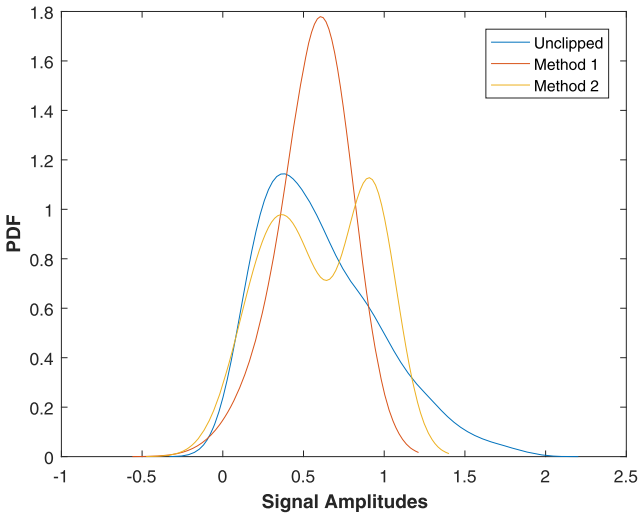

FIGURE 4. PDF distribution of signal amplitudes when clipped using Methods 1 and 2.

In Fig. 4, the PDFs showing the amplitude distribution of the two styles of clipping are demonstrated. The unclipped OFDM signal amplitude by default follows the Rayleigh distribution with significantly very small fractions of the amplitudes existing above the mean - this is usually responsible for the high PAPR metric of unprocessed OFDM signals. PDFs showing larger concentration of amplitudes around the mean tend to uniform distribution and will attain the optimal PAPR performance. This property is achieved by the Method 1, hence works with better PAPR performance than Method 2 and the unclipped signals as shown in Fig. 4.

B. PROPOSED ICF MODEL - METHOD 3

Method 2 shows two peaks, the lower one corresponding to the conventional amplitude distribution achieved through Method 1 and the second peak corresponding to the peaks

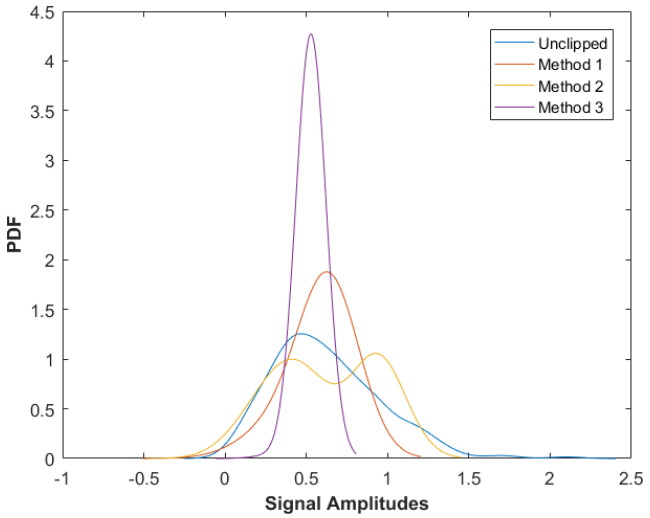

FIGURE 5. PDF distribution of signal amplitudes when clipped using Methods 1, 2 and 3.

obtained by scaling up all the mean amplitude by $\sqrt{\frac{\ell N}{P}}$ in (8). By this fact, it follows that, to achieve a perfect PAPR reduction of 0dB (i.e. PAPR = 1) involves two steps; 1) scale up all amplitudes smaller than $x_\dagger$ using (8) or force them to $x_\dagger$; 2) clip all amplitudes greater than $x_\dagger$ using (6). A problem with this scheme is that the resulting distortion noise is usually high leading to poor BER performance. As an open challenge therefore, we encourage the reader to explore optimal solution for maximizing the BER performance based on these two simple straightforward steps. By this method (i.e. Method 3), the amplitude distribution clusters more around the mean amplitude as shown in Fig. 5 compared to those in Methods 1 and 2.

III. METRICS FOR IMPROVING PERFORMANCE OF PROPOSED ICF MODELS

In this section, we present different performance improvement metrics for an OFDM system to enhance the performance of the proposed system models. All metric enhancement parameters described in this section fit into the evaluation of any of the three models presented above, however, we exemplify the procedures using Method 1 except where it is specifically stated otherwise.

A. PAPR OF OFDM SYSTEM

The PAPR is estimated as a ratio of maximum and average powers of an OFDM signal. For example, let us define the PAPR of an OFDM system as [9], [10], [21]

$$\text{PAPR} = \frac{\max\limits_{n=0,1,\cdots,\ell N-1}\left\{|x(n)|^2\right\}}{\frac{1}{\ell N}\sum\limits_{n=0}^{\ell N-1}\left\{|x(n)|^2\right\}} = \frac{\|\boldsymbol{x}\|_\infty^2}{\frac{1}{\ell N}\|\boldsymbol{x}\|_2^2} \tag{11}$$

where $\|\cdot\|_\infty$ represents ∞-norm and $\|\cdot\|_2 \leq \sqrt{\left(\sum|\cdot|^2\right)}$. Complementary cumulative distribution function (CCDF) is used to measure PAPR as

$$\text{CCDF} = \Pr\{\text{PAPR} > \gamma_o\} \tag{12}$$

where $\Pr\{\cdot\}$ is the probability of $\{\cdot\}$ and γ_o is the desired threshold. In PAPR reduction using ICFs, the in-band signal is distorted by the excess signal amplitudes which degrades BER performance. This can be measured by estimating the error vector magnitude (EVM) which measures the degree of deviation of a signal from its constellation point and can be expressed as [10]

$$\beta = \sqrt{\frac{\sum\limits_{n=0}^{N-1}\left|X(n)-\hat{X}(n)\right|^2}{\sum\limits_{n=0}^{N-1}|X(n)|^2}} = \frac{\left\|X(n)-\hat{X}(n)\right\|_2}{\|X(n)\|_2} \tag{13}$$

where $X(n)$ is the frequency-domain equivalent of the unclipped signal and $\hat{X}(n)$ is the frequency-domain equivalent of the clipped signal. It follows that reducing the error vector $\left\|X(n)-\hat{X}(n)\right\|_2$ in (13) will reduce the PAPR and also reduce the number of iterations involved. Based on this, next we explore the adaptive optimization technique described in [5] for increasing the PAPR performance by reducing the error vector demonstrated in Section III-B.

The estimation of the error vector helps to minimize the distortion noise. Thus, the removal of the distortion noise minimizes peak regrowth (which amplifies the PAPR and leads to too many iterations), thus minimizes the number of iterations. In this work, we achieve the removal of the distortion noise through optimization process as described in the next section.

B. ADAPTIVE OPTIMIZATION OF PROPOSED ICF SCHEME

This optimization technique is based on reducing the error vector so that β in (13) can be minimized; earlier studies involving EVM and convex optimization in PAPR reduction are available in the literature [9], [10], [21]–[23]. To reduce the EVM and the number of ICF iterations, $C = \left\|X(n)-\hat{X}(n)\right\|_2$ must be reasonably small. Such problem can be solved by constructing an optimal filter as [10] or by constructing a suitable PAPR reduction vector as in [9]. The optimal filter method involves running a special software, the CVX tool, while the PAPR vector method can be solved in closed form, thus the latter is preferred. Since the process is iterative, we cast the problem unto [9] method, then the problem becomes

$$\min_{C_m\in\mathbb{C}^N} \quad \beta = \frac{\|C_m\|_2}{\|X\|_2} \tag{14a}$$

subject to

$$\boldsymbol{c}_{m+1} = \text{IFFT}\,(C)_{1\times\ell N} \tag{14b}$$

$$|\boldsymbol{x}_m - \boldsymbol{c}_{m+1}| \leq x_\dagger^m \tag{14c}$$

where $x_\dagger^m$ denotes that (4a) must be updated at each iteration. By squaring both sides of (14), the LM optimization approach

$\mathcal{L}(C_m, \lambda)$ to the problem can be written as

$$\mathcal{L}(C_m, \lambda) = \frac{\|C_m\|_2^2}{\|\boldsymbol{x}\|_2^2} + \lambda\left(|\boldsymbol{x}_m - c_{m+1}|^2 - \left(x_\dagger^m\right)^2\right) \quad (15)$$

where λ is the Lagrange multiplier. From the LM optimization approach [5], the closed form solution can be found as

$$C_m = \frac{1}{\sqrt{N}}\left(|\boldsymbol{x}_m| - x_\dagger^m\right)e^{j\theta_m} \quad (16)$$

where θ_m is the phase of the signal cast back unto the reduction vector. This solution is an optimal PAPR reduction scheme that also minimizes the number of iterations. We have shown earlier in [5] that there exists a new peak and also a new average power at each iteration which requires iteratively recalculating the new clipping threshold [13]. The adaptive ICF approach in [13] is not optimized, thus we extend our solution of (16) to the adaptive approach reported in [5] which computes a new $x_\dagger^m$ using (4a) at each iteration.

C. COMPENSATING FOR THE NONLINEARITY OF THE PAPR REDUCTION SCHEME

From the foregoing discussion, it can be observed that the PAPR reduction solution is a nonlinear solution. Meanwhile, from Bussgang theorem [8], [24], [25], the output amplitude-distorted signals can be expressed as

$$\hat{\boldsymbol{x}}(n) = \alpha\boldsymbol{x}(n) + \boldsymbol{d}(n) \quad (17)$$

where α is the attenuation factor and $\boldsymbol{d}(n)$ is the uncorrelated distortion noise. The average power dissipated by the output clipped signal can be described as

$$P_{out} = \mathbb{E}\left\{\left|\hat{\boldsymbol{x}}(n)\right|^2\right\} \quad (18)$$

and the average distortion power can also be expressed in terms of the signal attenuation power as

$$P_d = \mathbb{E}\left\{|\boldsymbol{d}(n)|^2\right\} = P_{out} - P_{att} \quad (19)$$

while the attenuated signal power can be expressed as

$$P_{att} = \mathbb{E}\left\{|\alpha\boldsymbol{x}(n)|^2\right\} = \alpha^2\mathbb{E}\left\{|\boldsymbol{x}(n)|^2\right\} \quad (20)$$

Finally, the signal-to-distortion noise power ratio (SDR) can be represented as (21)

$$\text{SDR} = \frac{P_{att}}{P_d} = \frac{P_{att}}{P_{out} - P_{att}} \quad (21)$$

Thus, the problem now translates to deriving the analytical closed-form expression for the attenuation factor and plugging it into (17). To do that, let us express the attenuation factor [26], [27] as follows

$$\alpha = \frac{1}{\sigma_x^2}\int_0^\infty \Omega(x(n))\, x_0 f_{|x(n)|}dx \quad (22)$$

where x_0 is the discrete envelope of the unclipped signal $x(n)$, $\Omega(x(n))$ is the nonlinear amplitude distorting function and $f_{|x(n)|}$ is the PDF of the unclipped signal which usually follows Rayleigh distribution. Let the output clipped signal be represented in terms of the input signal and clipping (amplitude distortion) noise

$$s(n) = x(n) + b(n) \quad (23)$$

such that the output power can be expressed as

$$\sigma_s^2 = \sigma_x^2 + 2\mathbb{E}\left\{b^*(n)x(n)\right\} + \sigma_b^2 \quad (24)$$

where $b(n)$ is the clipping noise and $(\cdot)^*$ is the complex conjugate operator. Supposing that the input signal is well-normalized such that it maintains unit power $\sigma_s^2 = \sigma_x^2 = 1$, then

$$\sigma_b^2 = -2\mathbb{E}\left\{b^*(n)x(n)\right\} \quad (25)$$

The nonlinear amplitude distorting function is given by clipping function in (6) and the attenuation factor can be achieved in simulation (see [27], [28]) as

$$\alpha = \frac{\mathbb{E}\left[\boldsymbol{x}(n)\cdot\hat{\boldsymbol{x}}^*(n)\right]}{\mathbb{E}\left[|\boldsymbol{x}(n)|^2\right]} \quad (26a)$$

$$= 1 + \frac{\mathbb{E}\left[b^*(n)\cdot x(n)\right]}{\sigma_x^2} \quad (26b)$$

where $\sigma_x^2 = \mathbb{E}\left[|\boldsymbol{x}(n)|^2\right]$, $\mathbb{E}[\cdot]$ is the statistical expectation value operator and $\hat{\boldsymbol{x}}(n)$ is the output clipped signal in (6). Substituting for cross-correlation between the distortion noise and the original signal,

$$\alpha = 1 - \frac{\sigma_b^2}{2\sigma_x^2} \quad (27)$$

From (27), $\alpha \to 1$ as $\sigma_b^2 \to 0$ in which case, a compensation is not required. However, this is not realistically the case during nonlinear amplitude processing as $\sigma_b^2 \neq 0$.

D. NONLINEAR TRANSMISSIONS OVER HIGH POWER AMPLIFIER

The objective of PAPR reduction is to ensure that OFDM signals operate below the saturation regions of HPAs. To assess the performance of the proposed PAPR scheme over HPA, we consider a solid-state power amplifier (SSPA) that operates on the output clipped signal as follows [27]

$$D\left(\hat{\boldsymbol{x}}(n)\right) = F(\rho_n)\, e^{j(\phi_n + \Phi(\rho_n))} \quad \forall n = 0, 1, \cdots, \ell N - 1 \quad (28)$$

where $F(\cdot)$ and $\Phi(\cdot)$ are the AM/AM and AM/PM converters respectively of $\hat{\boldsymbol{x}}(n) = \left|\hat{\boldsymbol{x}}(n)\right| e^{j\arg\{\hat{\boldsymbol{x}}(n)\}} = \rho_n e^{j\phi_n}$. We limit our studies to amplitude distortion and so, the phase distortion is thus negligible [11]. Now, consider an AM/AM SSPA operating over the output clipped signal as follows

$$\boldsymbol{x}_{pa}(n) = F(\rho_n) \quad (29a)$$

$$= \frac{g_0\left(\hat{\boldsymbol{x}}(n)\right)}{\left(1 + \left(\frac{g_0(\hat{\boldsymbol{x}}(n))}{A_{sat}}\right)^{2q}\right)^{\frac{1}{2q}}} e^{j\phi_n} \quad (29b)$$

$$= \alpha_{pa}\hat{\boldsymbol{x}}(n) + \boldsymbol{d}_{pa}(n) \quad (29c)$$

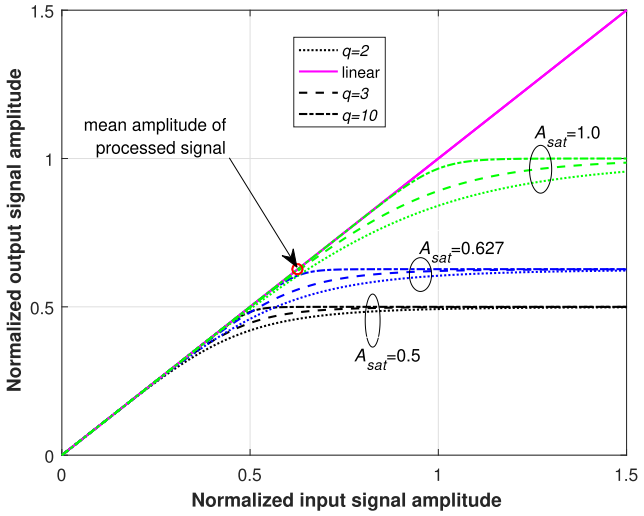

FIGURE 6. Nonlinear solid-state power amplifier showing different saturation levels including the mean amplitude processed.

where $g_0\left(\hat{x}(n)\right) = \rho_n$, $A_{sat} = \sqrt{P_T}$ is the input saturation level with P_T as the saturation power and q determines the output sharpness parameter. Thus, model (29) induces some nonlinear distortion into the signal causing further in-band distortion in addition to the ICF. In Fig. 6, three different saturation levels are exemplified. It follows that the performance of the amplifier on the input signal depends on the input saturation level of the HPA. In this study, the input signal is shown (with red circle) to exist at $\approx$ 0.6 mean amplitude which is reasonably lower than saturation level of the HPA at $A_{sat} = 1.0$ and reasonably high when $A_{sat} = 0.5$. In practical HPAs, output sharpness parameter is usually set at $q = 2$ or 3 [11] and this is adopted in this study setting $q = 3$.

E. COMPENSATING FOR NONLINEAR TRANSMISSION OVER HPA

Since clipping and HPA processes are independent, we analyze the signal transmission behaviour and compensations separately. Both ICF and HPA are independent nonlinear processes; thus we require to compensate the signal as already performed in the case of ICF in Section III-C. Now, by passing the output clipped signal over an AWGN channel, the received signal can be expressed as

$$\boldsymbol{r}(n) = \hat{\boldsymbol{x}}(n) + \boldsymbol{w}(n) \tag{30}$$

where $\boldsymbol{w} \sim \mathcal{CN}\left(0, \sigma_w^2\right)$ is the additive white Gaussian noise (AWGN) with variance $\sigma_w^2 = N_0/2$, $\mathcal{C}$ denotes that $\boldsymbol{w}$ is both circularly symmetric and complex [29], N_0 is the value of the one-sided power spectral density (PSD) of the noise. Then, considering the effects of the HPA and using (17) in (30), the output result can be expressed as

$$\begin{aligned}\boldsymbol{r}(n) &= \alpha_{pa}\boldsymbol{x}_{pa}(n) + \boldsymbol{d}_{pa}(n) + \boldsymbol{w}(n) \\ &= \alpha_{pa}\boldsymbol{x}_{pa}(n) + \boldsymbol{w}_d(n)\end{aligned} \tag{31a}$$

where $\boldsymbol{x}_{pa}(n)$ is the output signal from HPA in (29) scaled by the ICF attenuation factor from the ICF process in (26) and

$$\boldsymbol{w}_d(n) = \boldsymbol{d}_{pa}(n) + \boldsymbol{w}(n). \tag{31b}$$

From (17), if the attenuation factor can be estimated, then compensating for this before transmission can improve the system performance such as

$$\hat{\boldsymbol{x}}_{pa}(n) = \frac{\boldsymbol{x}_{pa}(n)}{\alpha_{pa}} = \hat{\boldsymbol{x}}(n) + \frac{\boldsymbol{d}_{pa}(n)}{\alpha_{pa}} \tag{32}$$

If the distortion noise due to HPA can be estimated, and scaled by the attenuation factor due to HPA, then the signal integrity can be improved such that the transmitted signals become

$$\bar{\boldsymbol{x}}(n) = \hat{\boldsymbol{x}}_{pa}(n) - \frac{\boldsymbol{d}_{pa}(n)}{\alpha_{pa}} = \hat{\boldsymbol{x}}(n) + \frac{\boldsymbol{d}_{pa}(n)}{\alpha_{pa}} - \frac{\boldsymbol{d}_{pa}(n)}{\alpha_{pa}} \tag{33a}$$

$$\Rightarrow \bar{\boldsymbol{x}}(n) = \boldsymbol{x}(n) + \boldsymbol{d}(n). \tag{33b}$$

Similarly, if the distortion noise due to ICF can be estimated, then the signal integrity can also be increased; this is achieved from error vector in (16). Unfortunately, applying compensation after passing the signal through AWGN channel will amplify the noise in (33) such as in

$$\bar{\boldsymbol{x}}_{pa}(n) = \frac{\boldsymbol{r}(n)}{\alpha_{pa}} \tag{34}$$

$$= \boldsymbol{x}_{pa}(n) + \frac{1}{\alpha_{pa}}\left(\boldsymbol{d}_{pa}(n) + \boldsymbol{w}(n)\right). \tag{35}$$

We follow the regime of Section III-C also to compensate the signal before passing it through the AWGN channel. Generally, the attenuation factor α can be determined from estimating the clipping ratio, γ_o and plugging it into [27], [30]

$$\alpha = 1 - \exp\left(-\gamma_o^2\right) + \sqrt{\frac{\pi}{4}}\gamma_o \operatorname{erfc}\left(\gamma_o^{\frac{1}{2}}\right) \tag{36}$$

where $\gamma_o = \frac{x_\dagger}{\sqrt{P_{av}}}$, $P_{av} = \frac{1}{\ell N}\sum_{n=0}^{\ell N-1}|x(n)|^2$ and $\operatorname{erfc}(\cdot)$ is the complementary error function. Unfortunately, (36) holds for soft limiter [27], in other words the case in (29), when $q \to \infty$ [11].

Then, the correlation coefficient of the distorted and original signal, $\mathcal{R}_{pa}$, which minimizes the error in $\mathbb{E}\left[\left|\boldsymbol{x}(n) - \mathcal{R}_{pa}\bar{\boldsymbol{x}}^*(n)\right|^2\right]$ after power amplification can be written as [8]

$$\mathcal{R}_{pa} = \frac{\mathbb{E}\left[\boldsymbol{x}(n)\cdot\bar{\boldsymbol{x}}^*(n)\right]}{\mathbb{E}\left[|\boldsymbol{x}(n)|^2\right]} \tag{37}$$

where $\bar{\boldsymbol{x}}(n)$ is the HPA compensated output signal after the SSPA-HPA output signal from (29a) that is passed through an AWGN channel. The result (37) is only the compensation due to the effect of HPA; when the system operates only with consideration to ICF (i.e. ignoring HPA) the compensation in (37) reduces to only (26b). We report our results for the unclipped, clipped without the MMSE compensation and clipped with MMSE compensation in Sections IV and II-A.

IV. RESULTS AND DISCUSSIONS

Since the proposed technique does not use a preset clipping ratio, it is not fair to compare both proposed schemes with ICF which seeks to attain a target PAPR threshold. However, at the transmitter, we generate $N = 128$ random data and pass these through QPSK modulator as shown in Fig 1. The resulting symbols are then oversampled 4-times which subtends an over-sized 512 IFFT/FFT points which are then used to transform the signal into time-domain using IFFT-block. Here, we estimate the mean amplitude of the signal as described in (4a). Using the mean amplitude, the excess signal amplitude above the mean are clipped off and using the PAPR reduction vector in (16), we optimize the iterations and improve the PAPR performance. The output clipped signal is then compensated using (26), then passed through HPA and compensated using (37) before transmission. The resulting signal is then passed through an AWGN channel with zero mean and variance σ_w^2. At the receiver, the received signal is then converted from serial to parallel, then transformed back into frequency domain and downsampled before QPSK demodulation. It must be noted that no error correction coding has been applied and no cyclic prefix is used as impulsive channel is not considered. To compare the output result with the originally transmitted data, we compare the received signal and the transmitted signal so that the BER can be estimated. Clearly, we evaluate the BER performance based on 1) adaptive optimized scheme and adaptive non-optimized scheme (without MMSE); 2) adaptive optimized scheme and non-optimized scheme (with MMSE).

A. PERFORMANCE EVALUATION OF THE PROPOSED ICF SCHEME (METHOD 1) WITH AND WITHOUT OPTIMIZATION

In the set of results in our investigation, we evaluate the performance of the proposed PAPR reduction scheme when operated with and without optimization. Optimization helps to maximize the PAPR reduction performance with minimal iterations by constructing a suitable PAPR reduction vector as described in Section III-B. In Fig. 7, the proposed PAPR reduction model greatly reduces the PAPR of the conventional OFDM system by 8dB at 3 iterations. By applying optimization, the PAPR is further reduced by 3.6 dB.

It is well-known that PAPR reduction is achieved at the expense of the increased error probability in the received signal. For example, the proposed ICF PAPR reduction scheme achieves the presented PAPR reduction indices at the cost of reduced BER performance in comparison to the unmodified OFDM system due to in-band distortion noise. The BER metric on the other hand reflects the measure of how much distortion noise has been injected into the transmitted signal which causes deviation from the desired symbol constellation positions as shown in Fig. 8. However, we improve the BER performance by reducing the noise overhead before transmitting the PAPR reduced signal using the MMSE correction. To achieve this, we compensate the PAPR reduced

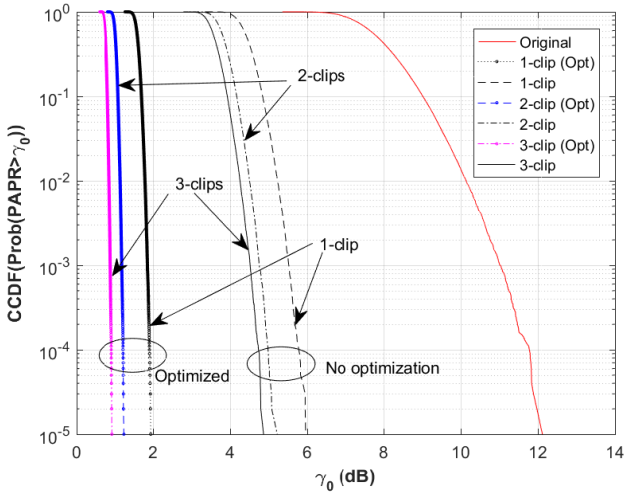

FIGURE 7. PAPR Performance of the proposed new ICF approach in Method 1 for reducing the PAPR of OFDM systems with and without optimization.

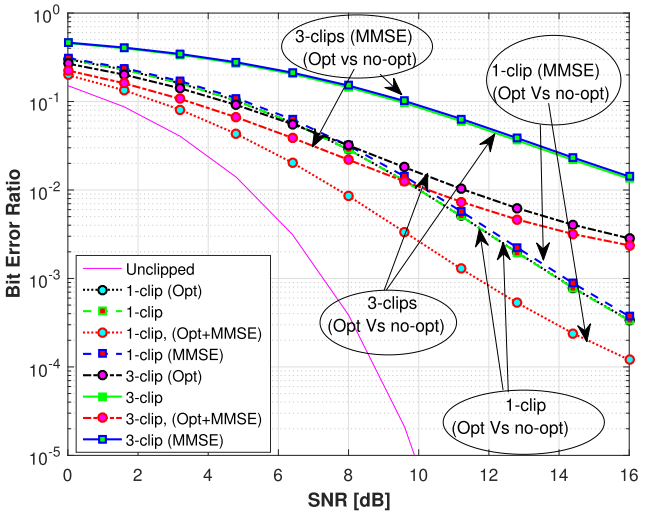

FIGURE 8. BER Performance of the proposed new ICF approach for reducing the PAPR of OFDM systems ($\ell = 4$, $N = 128$) with and without optimization.

signal using the adaptively determined post-PAPR reduction factor as described in (26b) before transmission. In Fig. 8, the MMSE compensation slightly reduces to improve the BER; this is more significant in the optimized scheme. The optimized and non-optimized performed alike in terms of BER with 1 iteration. With 3 iterations, the optimized scheme achieved 5dB better than non-optimized version at 10^{-2} BER. When MMSE is applied, with 1 iteration, the optimized version achieved 2.5dB at 10^{-3} BER while with 3 iterations the optimized version achieved 6dB better than the non-optimized version at 10^{-2} BER. Next, comparing MMSE and with no MMSE, there is 2.5dB gain within the optimized scheme and 1dB at 3 iterations at 10^{-2} BER but provides insignificant gain in all the non-optimized schemes. In 1 iteration, comparing optimized and non-optimized

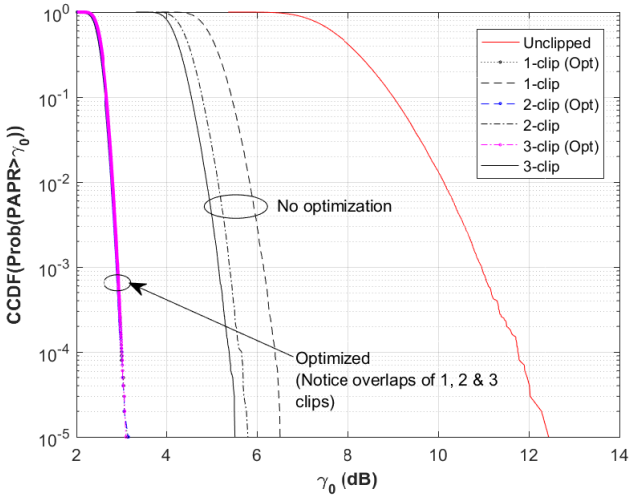

FIGURE 9. PAPR performance of proposed ICF PAPR Method 2 comparing adaptive optimized and adaptive non-optimized schemes ($\ell = 4$, $N = 128$).

schemes, the optimized achieved 2dB gain at 10^{-3} BER and over 4dB gain at 10^{-2} BER with 3 iterations (without MMSE). The MMSE improvement is due to the removal of noise vector before further processing and transmission.

B. PERFORMANCE EVALUATION OF PAPR AND BER USING METHOD 2

Recall the signal transmission over the AWGN channel in explained Section III-E. We can express the received signal as follows

$$y(n) = \alpha_{pa}\hat{\boldsymbol{x}}(n) + \boldsymbol{d}_{pa}(n) + \boldsymbol{w}(n), \quad \forall n = 1, \cdots, \ell N \qquad (38)$$

where $d_{pa}(n)$ is the new distortion component of the HPA. The received SNR after HPA can be described as follows

$$\gamma = 10\log_{10}\left(\alpha^2\left(\frac{\sigma_x^2}{\sigma_w^2}\right)\right) \qquad (39)$$

where σ_x^2 is the input signal power and σ_w^2 is the overall noise power. Substituting for the attenuation power from (27) into (39), we obtain

$$\gamma = 10\log_{10}\left(\left(1 - \frac{\sigma_b^2}{2\sigma_x^2}\right)^2 \times \left(\frac{\sigma_x^2}{\sigma_w^2}\right)\right) \qquad (40)$$

Obviously, reducing the attenuation factor power, namely σ_b^2 in (40) increases the SNR and thus improves the BER. One of the ways of doing this is by reducing the depth of clipping of the signal. For example, due to the depth of clipping in the proposed ICF method above, the in-band distortion is very high which suggests an increased EVM and highly degraded BER. In this section, the performance enhancement is achieved through our proposed Method 2 described in Section II-A.

The PAPR performances of the second procedure are presented in Fig. 9. Clearly, the PAPR of the original signal is well reduced. Also, observe that the optimized scheme outperforms the non-optimized method while achieving optimal performance in 1 iteration. However, when the result of Method 2 in Fig. 9 is compared to Method 1 in Fig. 7, it can be found that the PAPR performance is degraded. The reason can be straightforwardly obtained from comparing (8) and (4a) which determines the amplitude threshold required to be clipped. In (4a) criteria, more amplitudes are clipped while in (8) less number of amplitudes are clipped thus lowering the PAPR performance.

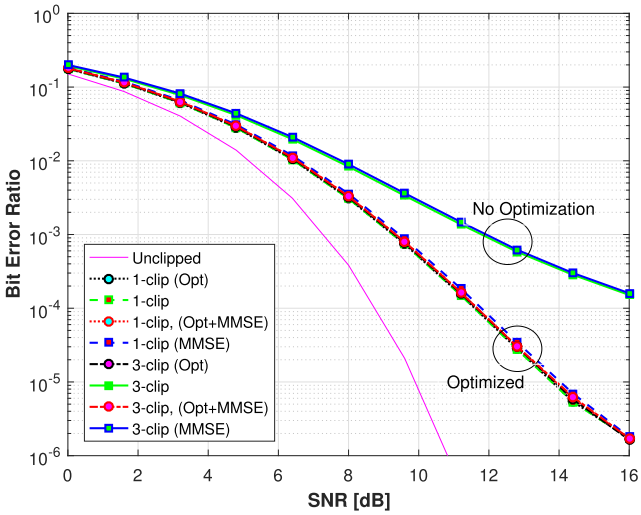

FIGURE 10. BER Performance of adaptive optimized and adaptive non-optimized PAPR reduction scheme (Method 2).

In terms of BER performance, we present the corresponding performance of the proposed Method 2 in Fig. 10. Now, since there are lower number of amplitudes to be clipped in (8), then there will be correspondingly less amplitude distortions which will translate into better BER performance. This is true as shown in Fig. 10 where Method 2 achieves increased BER performance.

C. PERFORMANCE EVALUATION OF METHOD 3

Obviously, the PAPR performance of the third method is significant in Fig. 11 and better than earlier two schemes due to its ability to achieve a better PDF distribution with most amplitudes centering around the mean. Comparing Methods 1 and 2 in terms of PAPR performance, Method 1 outperforms Method 2 in terms of PAPR for all iterations. This obviously follows from the fact that the amplitudes of some signals are selectively enhanced while others are selectively reduced (and all towards a uniform distribution) which also enhanced the PAPR threshold. The BER performances of all the schemes are combined and presented in Fig. 12 for ease of reference and comparison with Method 2 achieving the best BER performance followed by Method 1.

D. PSD PERFORMANCE EVALUATION OF METHODS 1, 2 AND 3

Although the out-of-band emission reduction of OFDM systems due to PAPR reduction is not the key focus of this

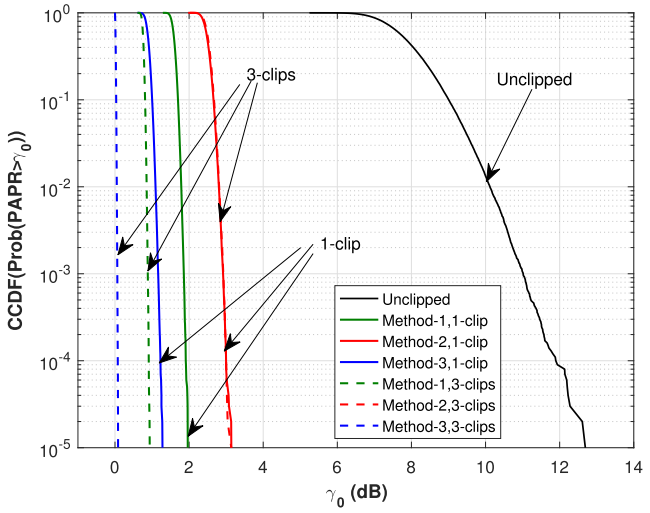

FIGURE 11. Performance evaluation of three different ICF styles based on the PDF distribution of the amplitudes of OFDM signals (with optimization).

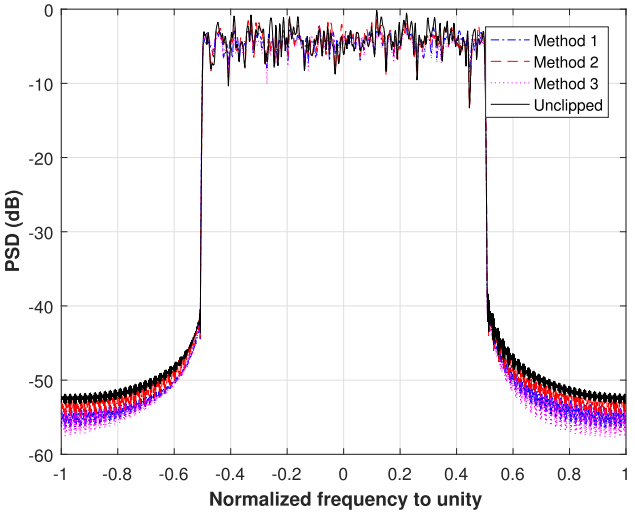

FIGURE 13. Performance comparison of power spectral density for the proposed three ICF schemes with unclipped OFDM signals.

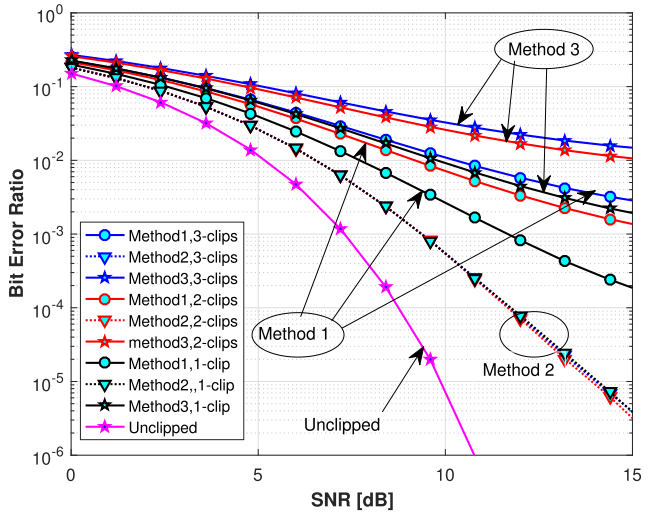

FIGURE 12. BER Performance of proposed three methods of PAPR reduction based on iterative clipping and filtering (with optimization and one-level MMSE).

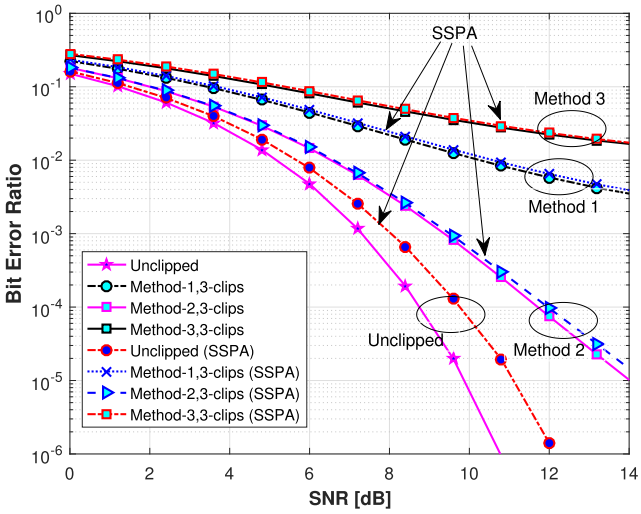

FIGURE 14. BER Performances over HPA for the two proposed BER reduction methods (all with the two-level nonlinear MMSE compensations).

study (see [31, and references therein]), we show some improvement achieved when the proposed scheme is applied. We evaluate the PSD of the proposed schemes with the unclipped as shown in Fig. 13. Compared to the unclipped, the proposed ICF schemes achieve lower out-of-band interference (OBI) showing 4.47dB, 1.68dB and 3.23 dB gains for Methods 1, 2 and 3 respectively, in the PSD plots.

E. PERFORMANCE EVALUATION OF BER OF METHODS 1, 2 AND 3 WHEN USING HPA

We explore the performance of the proposed schemes over solid-state power amplifier with characteristic input saturation amplitude level of 1. The idea of reducing the PAPR of OFDM system is to ensure that the highest amplitude does not (or that only minimal number of amplitudes) appear within the nonlinear region of the HPA as this can induce amplitude distortion into the signal and reduces the BER performance. For the two proposed schemes emerging from the foregoing discussions, we perform the evaluation of their BERs over the SSPA described in Section III-D as presented in Fig. 14. The results show that passing the signal through SSPA does not greatly impact the BER performance of all the proposed methods due to reduced amplitude peaks. However, observe that the BER of unclipped signal is largely degraded as depicted in Fig. 14. In fact, compensating for the HPA nonlinear distortion improves the BER performance of all methods such that BER degradation is negligible when passed over the HPA. In general, Method 2 achieves the best BER performance both when working with and without SSPA. While performing well with just 1 iteration, it also achieves considerable reduction in the PAPR performance, however performs worse than Methods 1 and 3. The Method 3 achieves

the best performing PAPR performance but the worst BER; this, we have enumerated an open challenge on finding optimal techniques that can improve the BER performance. Finally, Method 2 achieves the worst PAPR performance but the best BER. It therefore follows that the choice of the technique to be deployed depends on the system designer and on the intended output performance. Meanwhile, for best BER performance and fair PAPR, we recommend the use of Method 2.

V. CONCLUSION

We have, in this paper, presented three new methods of handling the PAPR reduction problem in OFDM systems based on clipping and filtering. The proposed methods are based on transforming the amplitude distribution of conventional OFDM system to uniform distribution. Using the mean amplitude as a reference amplitude, we clip excess amplitudes to approach uniform distribution. A second approach scales the mean with reference to the excess amplitudes which achieves better BER performance than the previous. Combining the ideas gained from the first two, we proposed a third method which amplifies the amplitudes distributed below the mean, then clipping the all amplitudes above the mean to achieve 0dB PAPR in 3 iterations. To reduce the number of iterations involved, we applied the Lagrange multiplier optimization technique to reduce the distortion noise which impacted the PAPR and the BER also. To compensate for the nonlinear distortions, we applied MMSE after ICF and passing the signal through HPA. This further improved the BER performance. The proposed schemes can be further improved by finding optimal technique to reduce in-band distortion noise. Finally, we have shown that the proposed methods also achieve lower OBI compared to the unclipped scheme.

REFERENCES

[1] K. O. O. Anoh, J. M. Noras, R. A. Abd-Alhameed, S. M. Jones, and K. N. Voudouris, "A new approach for designing orthogonal wavelets for multicarrier applications," *AEU-Int. J. Electron. Commun.*, vol. 68, no. 7, pp. 616–622, Jul. 2014.

[2] K. O. Anoh, R. Abd-Alhameed, J. Noras, and S. Jones, "Wavelet packet transform modulation for multiple input multiple output applications," *Int. J. Comput. Appl.*, vol. 63, no. 7, pp. 46–51, Feb. 2013.

[3] G. Wunder, R. F. H. Fischer, H. Boche, S. Litsyn, and J.-S. No, "The PAPR problem in OFDM transmission: New directions for a long-lasting problem," *IEEE Signal Process. Mag.*, vol. 30, no. 6, pp. 130–144, Nov. 2013.

[4] Y. Rahmatallah and S. Mohan, "Peak-to-average power ratio reduction in OFDM systems: A survey and taxonomy," *IEEE Commun. Surveys Tuts.*, vol. 15, no. 4, pp. 1567–1592, 4th Quart., 2013.

[5] K. Anoh, C. Tanriover, and B. Adebisi, "On the optimization of iterative clipping and filtering for PAPR reduction in OFDM systems," *IEEE Access*, vol. 5, pp. 12004–12013, Jun. 2017.

[6] J. Armstrong, "Peak-to-average power reduction for OFDM by repeated clipping and frequency domain filtering," *Electron. Lett.*, vol. 38, no. 5, pp. 246–247, Feb. 2002.

[7] T. Jiang, Y. Yang, and Y.-H. Song, "Exponential companding technique for PAPR reduction in OFDM systems," *IEEE Trans. Broadcast.*, vol. 51, no. 2, pp. 244–248, Jun. 2005.

[8] R. Yoshizawa and H. Ochiai, "Effect of clipping and filtering with distortionless PAPR reduction for OFDM systems," in *Proc. IEEE 82nd Veh. Technol. Conf. (VTC Fall)*, Sep. 2015, pp. 1–5.

[9] X. Zhu, W. Pan, H. Li, and Y. Tang, "Simplified approach to optimized iterative clipping and filtering for PAPR reduction of OFDM signals," *IEEE Trans. Commun.*, vol. 61, no. 5, pp. 1891–1901, May 2013.

[10] Y.-C. Wang and Z.-Q. Luo, "Optimized iterative clipping and filtering for PAPR reduction of OFDM signals," *IEEE Trans. Commun.*, vol. 59, no. 1, pp. 33–37, Jan. 2011.

[11] A. K. Gurung, F. S. Al-Qahtani, A. Z. Sadik, and Z. M. Hussain, "One-iteration-clipping-filtering (OICF) scheme for PAPR reduction of OFDM signals," in *Proc. Int. Conf. Adv. Technol. Commun.*, Oct. 2008, pp. 207–210.

[12] C. Sharma, P. K. Sharma, S. K. Tomar, and A. K. Gupta, "A modified iterative amplitude clipping and filtering technique for PAPR reduction in OFDM systems," in *Proc. Int. Conf. Emerg. Trends Netw. Comput. Commun.*, Apr. 2011, pp. 365–368.

[13] B. M. Lee and Y. Kim, "An adaptive clipping and filtering technique for PAPR reduction of OFDM signals," *Circuits Syst. Signal Process.*, vol. 32, no. 3, pp. 1335–1349, Jun. 2013.

[14] S.-S. Jeng and J.-M. Chen, "Efficient PAPR reduction in OFDM systems based on a companding technique with trapezium distribution," *IEEE Trans. Broadcast.*, vol. 57, no. 2, pp. 291–298, Jun. 2011.

[15] T. Jiang and G. Zhu, "Nonlinear companding transform for reducing peak-to-average power ratio of OFDM signals," *IEEE Trans. Broadcast.*, vol. 50, no. 3, pp. 342–346, Sep. 2004.

[16] Y. Wang, J. Ge, L. Wang, J. Li, and B. Ai, "Nonlinear companding transform for reduction of peak-to-average power ratio in OFDM systems," *IEEE Trans. Broadcast.*, vol. 59, no. 2, pp. 369–375, Jun. 2013.

[17] A. K. Gurung, F. S. Al-Qahtani, A. Z. Sadik, and Z. M. Hussain, "Power savings analysis of clipping and filtering method in OFDM systems," in *Proc. Austral. Telecom. Netw. Appl. Conf. (ANTAC)*, Dec. 2008, pp. 204–208.

[18] K. Anoh, B. Adebisi, and M. Hammoudeh, "A comparison of ICF and companding for impulsive noise mitigation in powerline communication systems," in *Proc. Int. Conf. Future Netw. Distrib. Syst.*, Jul. 2017.

[19] X. Wang, T. T. Tjhung, and C. S. Ng, "Reduction of peak-to-average power ratio of OFDM system using a companding technique," *IEEE Trans. Broadcast.*, vol. 45, no. 3, pp. 303–307, Sep. 1999.

[20] J. Hou, J. H. Ge, and J. Li, "Trapezoidal companding scheme for peak-to-average power ratio reduction of OFDM signals," *Electron. Lett.*, vol. 45, no. 25, pp. 1349–1351, Dec. 2009.

[21] Y.-C. Wang, J.-L. Wang, K.-C. Yi, and B. Tian, "PAPR reduction of OFDM signals with minimized EVM via semidefinite relaxation," *IEEE Trans. Veh. Technol.*, vol. 60, no. 9, pp. 4662–4667, Nov. 2011.

[22] A. Aggarwal and T. H. Meng, "Minimizing the peak-to-average power ratio of OFDM signals using convex optimization," in *Proc. IEEE GLOBECOM*, vol. 4. Dec. 2003, pp. 2385–2389.

[23] A. Aggarwal and T. H. Meng, "A convex interior-point method for optimal OFDM PAR reduction," in *Proc. IEEE ICC*, vol. 3. May 2005, pp. 1985–1990.

[24] P. Banelli. (Nov. 2011). "Non-linear transformations of Gaussians and Gaussian-mixtures with implications on estimation and information theory." [Online]. Available: https://arxiv.org/abs/1111.5950

[25] J. Hou, J. Ge, D. Zhai, and J. Li, "Peak-to-average power ratio reduction of OFDM signals with nonlinear companding scheme," *IEEE Trans. Broadcast.*, vol. 56, no. 2, pp. 258–262, Jun. 2010.

[26] Y. Wang, L. H. Wang, J. H. Ge, and B. Ai, "An efficient nonlinear companding transform for reducing PAPR of OFDM signals," *IEEE Trans. Broadcast.*, vol. 58, no. 4, pp. 677–684, Dec. 2012.

[27] I. Gutman, I. Iofedov, and D. Wulich, "Iterative decoding of iterative clipped and filtered OFDM signal," *IEEE Trans. Commun.*, vol. 61, no. 10, pp. 4284–4293, Oct. 2013.

[28] M. Hu, Y. Li, W. Wang, and H. Zhang, "A piecewise linear companding transform for PAPR reduction of OFDM signals with companding distortion mitigation," *IEEE Trans. Broadcast.*, vol. 60, no. 3, pp. 532–539, Sep. 2014.

[29] R. G. Gallager, "Circularly-symmetric Gaussian random vectors," to be published. [Online]. Available: https://pdfs.semanticscholar.org/815e/637fafa233b44e2067f6ce345734012bd844.pdf

[30] Z. Kollár, L. Varga, B. Horváth, P. Bakki, and J. Bitó, "Evaluation of clipping based iterative PAPR reduction techniques for FBMC systems," *Sci. World J.*, vol. 2014, pp. 1–12, Jan. 2014.

[31] M. Mohamad, R. Nilsson, and J. van de Beek, "An analysis of out-of-band emission and in-band interference for precoded and classical OFDM systems," in *Proc. 21st Eur. Wireless Conf.*, May 2015, pp. 1–5.

KELVIN ANOH (S'11–M'15) received the B.Sc. degree (Hons.) in industrial physics from Ebonyi State University, Nigeria, in 2006, the M.Sc. degree in data telecommunications and networks from the University of Salford, U.K., in 2010, and the Ph.D. degree in telecommunications engineering from the University of Bradford, U.K., in 2015. Since 2016, he has been a Research Associate with Manchester Metropolitan University, U.K., where he was involved in an InnovateUK-EPSRC Project that received both the Knowledge Exchange Project and Outstanding knowledge Awards in 2016, respectively. His research interests are in the areas of signal processing and emerging communication technologies. He is a member of IET. He received the Best Paper Award at the University of Cambridge, U.K., in 2017 during the ICFNDS'17 Conference.

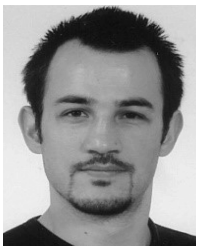

CAGRI TANRIOVER received the B.Sc. degree in electronics and communications engineering from Istanbul Technical University in 1997, and the M.Sc. degree in digital signal processing and the Ph.D. degree in communications systems from Lancaster University, U.K. He has an extensive industrial research and product development experience of over 14 years working as part of multidisciplinary teams in U.K., Turkey, and USA. He has successfully contributed to ETSI's TETRA TEDS Release 2 Standard, and is the co-inventor of the multifold turbo coding technique. He has published a number of articles in peer-reviewed journals and authored a number of international patents. His research interests include wireless communication, signal processing, and embedded systems.

BAMIDELE ADEBISI (M'06–SM'15) received the bachelor's degree in electrical engineering from Ahmadu Bello University, Zaria, Nigeria, in 1999, and the master's degree in advanced mobile communication engineering and the Ph.D. degree in communication systems from Lancaster University, U.K., in 2003 and 2009, respectively. He was a Senior Research Associate with the School of Computing and Communication, Lancaster University, from 2005 to 2012. He joined Manchester Metropolitan University, Manchester, in 2012, where he is currently a Reader in electrical and electronic engineering. He has involved in several commercial and government projects focusing on various aspects of wireline and wireless communications. He is particularly interested in research and development of communication technologies for electrical energy monitoring/management, transport, water, critical infrastructures protection, home automation, IoTs, and cyber physical systems. He has several publications and a patent in the research area of data communications over power line networks and smart grid. He is a member of IET.

MOHAMMAD HAMMOUDEH received the B.Sc. degree (Hons.) in computer communications from Arts, Sciences & Technology University, Lebanon, in 2004, the M.Sc. degree in advanced distributed systems from the University of Leicester in 2007, and the Ph.D. degree in computer science from the University of Wolverhampton in 2009. He is currently a Senior Lecturer in computer networks and security with the School of Computing, Mathematics and Digital Technology, Manchester Metropolitan University. He is the Co-Founder and a member of the FUture Networks and Distributed Systems RESEARCH GROUP. He is also the Founder and the Head of the MMU IoT Lab.